ACS APPLIED MATERIALS & INTERFACES

Research Article

www.acsami.org

Reprogrammable, Reprocessible, and Self-Healable Liquid Crystal Elastomer with Exchangeable Disulfide Bonds

Zhijian Wang,[†] Hongmiao Tian,[†,§] Qiguang He,[†] and Shengqiang Cai*[,†,‡]

[†]Department of Mechanical and Aerospace Engineering and [‡]Materials Science and Engineering Program, University of California, San Diego, La Jolla, California 92093, United States

[§]Micro- and Nano-technology Research Center, State Key Laboratory for Manufacturing Systems Engineering, Xi'an Jiaotong University, 28 Xianning Road, Xi'an 710049, P. R. China

Supporting Information

ABSTRACT: A liquid crystal elastomer (LCE) can be regarded as an integration of mesogenic molecules into a polymer network. The LCE can generate large mechanical actuation when subjected to various external stimuli. Recently, it has been extensively explored to make artificial muscle and multifunctional devices. However, in the commonly adopted two-step crosslinking method for synthesizing monodomain LCEs, the LCE needs to be well-cross-linked in the first step before stretching, which increases the disorder of mesogenic molecules in the final state of the LCE and makes it very challenging to fabricate the LCE of complex shapes. In this article, we developed a new LCE with disulfide bonds, which can be reprogrammed from the polydomain state to the monodomain state either through heating or UV illumination, owing to the rearrangement of the polymer network induced by the metathesis reaction of disulfide bonds. In addition, the newly developed LCE can be easily reprocessed and self-healed by heating. Because of the excellent reprogrammability as well as reprocessability of the LCE, we further fabricated LCE-based active micropillar arrays through robust imprint lithography, which can be hardly achieved using the LCE prepared previously. Finally, we showed an excellent long-term durability of the newly developed LCE.

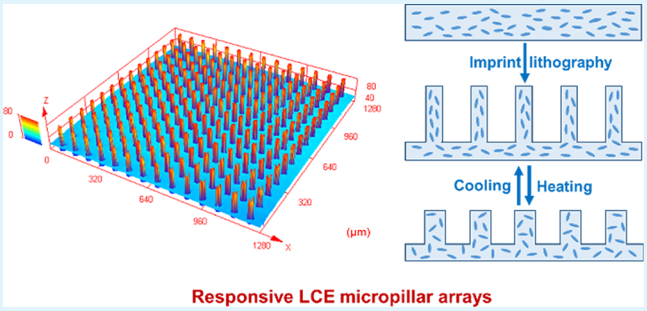

KEYWORDS: *liquid crystal elastomers, disulfide metathesis reaction, micropillar arrays, self-healing, reprocessing*

INTRODUCTION

A liquid crystal elastomer (LCE) can be synthesized by integrating mesogenic molecules into a polymer network. Because of its large actuation, high stretchability, and unique optomechanical response, the LCE has been extensively explored in a variety of applications ranging from artificial muscle[1−4] to mechanically tunable optical devices.[5−9] For example, Yu and his coworkers reported several kinds of photomechanical liquid crystalline actuators based on the photoisomerization effect of azobenzene molecules.[10−12] The photomechanical actuator has been used to convert light to electricity and to mimic various biological processes such as blooming and fading of flowers.

It is known that without a very cautious treatment, the LCE is usually obtained in the polydomain state at room temperature with a domain size of hundreds of nanometers. However, the monodomain LCE in which mesogenic molecules are well-aligned in one direction is often desired in many of its applications such as optomechanical coupling devices and soft actuators.[13−17] In the past decade, different methods have been developed to fabricate the monodomain LCE, including surface alignment,[18] application of the electric/magnetic field,[19−21] and mechanical stretching.[22,23] Among all these methods, the two-step crosslinking method has been widely adopted in synthesizing the monodomain LCE mainly because of its simplicity and robustness.[24] In the experiment, two cross-linking reactions with significantly different reaction rates are used in synthesizing monodomain LCEs. After the completion of the fast cross-linking reaction, uniaxial stress was applied onto a lightly cross-linked LCE sample. The slow cross-linking reaction then proceeded inside the stretched LCE. Finally, a monodomain LCE can be obtained, and all the mesogenic molecules orient toward the stretching direction. One well-known drawback of the method is that the LCE should be well-cross-linked to be stretchable in the first step, which increases the disorder of mesogenic molecules in the final state of the LCE and makes it very challenging to fabricate the LCE of complex shapes.[25] To eliminate these drawbacks, Ji et al. introduced exchangeable epoxy−acid bonds to replace permanent covalent bonds in LCE networks.[26−30] In their experiment, the as-prepared products are first in the polydomain state. Then, they obtain the monodomain LCE

Received: June 27, 2017
Accepted: September 7, 2017
Published: September 7, 2017

DOI: 10.1021/acsami.7b09246
ACS Appl. Mater. Interfaces XXXX, XXX, XXX−XXX

Scheme 1. Design of the Disulfide LCE and the Mechanistic Illustration of the Dynamic Network of the LCE under UV Irradiation or upon Heating

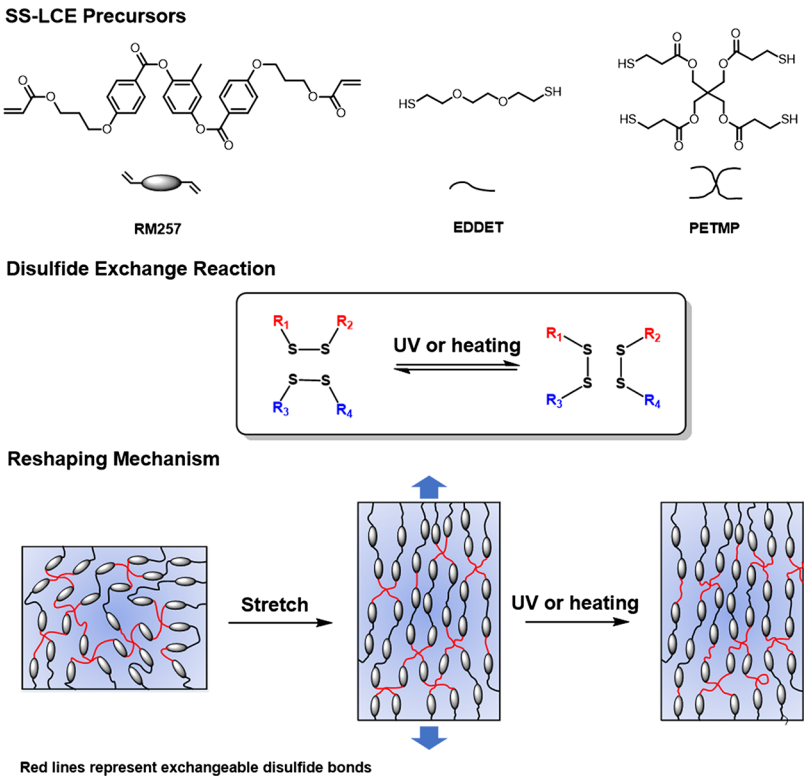

by simply stretching the sample at high temperature, under which the epoxy−acid polymer network can be rearranged by the transesterification exchange reaction. The strategy of incorporating dynamic covalent bonds makes the fabrication of the monodomain LCE much more reproducible and reliable.[31−33] However, a large amount of the catalyst is required for most reported dynamic covalent bonds. The catalysts may age during the storage, which makes the long-term functionality of the dynamic bonds system a well-recognized problem.[34] In addition, it is practically difficult to fabricate an LCE with a patterned orientation of mesogens through heating. Instead, the light-induced reaction has been extensively explored to fabricate a material with complex structures. For instance, using the photoalignment technique, White et al. precisely controlled the spatial distribution of the director of mesogenic molecules in the LCE and realized the transformation of the LCE from a flat sheet to a 3D structure.[35] Therefore, it is highly desired to develop a new LCE with an exchangeable dynamic bond whose property does not rely on the effectiveness of catalysts and its fabrication can be both optically and thermally controlled.

In recent years, a variety of exchangeable chemical reactions have been intensively studied in various polymeric systems, such as transesterification,[31−33] transcarbamoylation,[36,37] imine−amine exchange reaction,[38,39] disulfide metathesis,[40−44] olefin metathesis,[45,46] boronic ester exchange reaction,[47] and addition−fragmentation chain transfer reaction.[48,49] They have shown a great potential in making self-healable and reprocessible materials.[34] Among these exchangeable chemical reactions, disulfide metathesis can happen either under UV irradiation or upon heating without any catalysts or initiators.[50,51] Recent work has shown that the thiol−disulfide switches can also be triggered by adding oxidized or reduced reagents.[52] The unique dynamic property of disulfide bonds provides a new opportunity for the design and fabrication of the monodomain LCE. In this article, we developed a new type of LCE with disulfide bonds, which behaves like a thermoplastic material and can be reprogrammed from the polydomain to the monodomain state either under UV illumination or at high temperature in the absence of catalysts. In addition, it is also reprocessible and self-healable under high temperature. Compared to the previously reported reprogrammable LCEs, the LCE with disulfide bonds has three important advantages. First, the disulfide LCE can be reprogrammed temporarily and spatially at ambient temperature by UV irradiation. Second, complex microstructures can be easily fabricated on the surface of the disulfide LCE through imprint lithography to realize some novel functions. Third, unlike most other dynamic covalent bonds, the disulfide metathesis reaction can happen without a catalyst, which endows the disulfide LCE excellent long-term functionality. According to our knowledge, this is the first time that dynamic disulfide bonds are introduced into an LCE network to obtain a UV and thermally dual-reprogrammable LCE.

RESULTS AND DISCUSSION

In our experiment, the disulfide LCE was synthesized from three commercially available compounds, liquid crystal mesogen (1,4-bis-[4-(3-acryloyloxypropyloxy)benzoyloxy]-2-methylbenzene) (RM257), chain extender 2,2′-(ethylenedioxy)diethanethiol (EDDET), and cross-linker pentaerythritol tetrakis(3-mercaptopropionate) (PETMP) (Scheme 1). The detailed synthetic procedures are described in the section of Experimental Method, and the synthetic route is shown in Scheme S1.

DOI: 10.1021/acsami.7b09246
ACS Appl. Mater. Interfaces XXXX, XXX, XXX−XXX

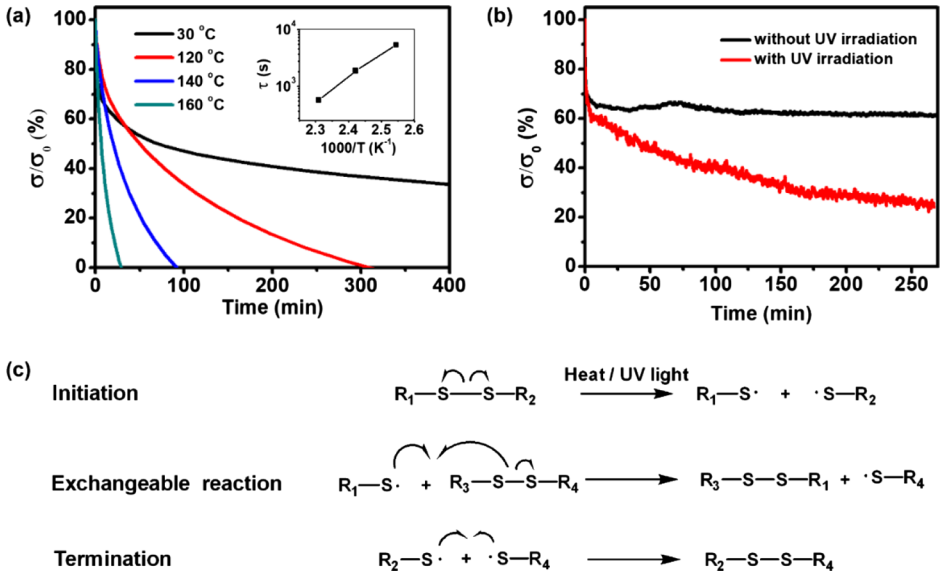

Figure 1. (a) Stress relaxation curves of SS-LCE-1 under several different temperatures with a fixed tensile strain of 20%. Inset: Relaxation time τ vs $1000/T$. (b) Stress relaxation curves of SS-LCE-1 with and without UV illumination under a fixed tensile strain of 100% and (c) mechanism of the disulfide metathesis reaction.

Briefly speaking, liquid crystal mesogen RM257 first reacted with flexible spacer EDDET via the Michael addition reaction to obtain an oligomer. EDDET was excessive to make sure that end groups of the oligomer are thiol groups. The degree of polymerization (DP) was calculated from the proton nuclear magnetic resonance (^{1}H NMR) spectrum of the oligomer (Figure S1). The signal in the ^{1}H NMR spectrum of the oligomer around 8.15 ppm corresponded to the protons at the benzyl ring of RM257, and its integration was set as 4. The signal around 3.6 ppm corresponded to the protons of $-CH_2-$ near the oxygen atoms of EDDET, whose integration was 9.69. The DP could be calculated as $8/(9.69 - 8) = 4.7$, which was consistent with the feed ratio between RM257 and EDDET. The oligomer was stable in the temperature range from 40 to 120 °C, as shown in the thermogravimetric analysis (TGA) result (Figure S2a). The isotropic transition temperature of the oligomer was around 56 °C, as determined by differential scanning calorimetry (DSC) analysis (Figure S2b). The cross-linker PETMP with equivalent thiol groups as oligomers, oxidized reagents hydrogen peroxide and catalyst sodium iodide were then added into the tetrahydrofuran (THF) solution of the oligomer. The gel formed after stirring for 24 h. The gel was then cut into small pieces and washed with 5 wt % sodium thiosulfate solution and water. After being dried in the oven, the obtained white gel pieces (Figure S3a) were hot-compressed into a thin film and marked as SS-LCE-1. Figure S3b shows the obtained yellow film with the smooth surface. It is well-known that thermosetting polymers cannot be reprocessed regardless of the processing technique applied because of their permanent covalent bonds. Herein, the disulfide bonds in the LCE became exchangeable via the metathesis reaction under high temperature, which enabled the application of thermal processing to convert small polymer pieces to a single polymer film. To confirm that the reprocessability of the newly designed LCE was originated from disulfide metathesis, we also synthesized another LCE without disulfide bonds using the same liquid crystal mesogens RM257, spacers EDDET, and cross-linkers PETMP by following the procedures reported previously.[53,54] In the control LCE sample, its cross-linking formed via the Michael addition reaction and photopolymerization of the excessive acrylate functional groups. The chopped LCE pieces were also subjected to hot compression under the same condition as before. Figure S3c,d show that an integrated LCE thin film could not be obtained. Such differences imply that the exchangeable reaction of disulfide bonds was vital to the reprocessability of the LCE designed by us.

We also used Fourier transform infrared spectroscopy (FT-IR) measurement to characterize the oxidation-induced cross-linking of the disulfide LCE as shown in Figure S4. The absorption band at 2550 cm^{-1} in the FT-IR spectrum of EDDET corresponded to the S−H stretching vibration of the end thiol groups.[43] The absorption band became weaker in the oligomers because of the Michael addition reaction between EDDET and RM257 and disappeared completely in the final LCE sample after oxidation by hydrogen peroxide, demonstrating that the thiol groups were totally oxidized into disulfide bonds in the LCE sample. The TGA result showed that the disulfide LCE did not decompose until the temperature reached 310 °C (Figure S5). The glass transition temperature of the disulfide LCE is around −4.5 °C determined by DSC (Figure S6). However, the nematic−isotropic transition temperature could not be identified in the DSC curve. The similar phenomenon was also reported by Yakacki et al. in the RM257-based LCE prepared via the two-stage polymerization method, and the isotropic temperature of the RM257-based LCE should be around 80 °C.[53,55]

We further conducted stress relaxation experiments on the synthesized LCE to study the exchangeable reaction of disulfide bonds. In the test, the LCE specimen (10 mm × 5 mm × 0.5 mm) was subjected to isostrain stress relaxation experiments on the dynamic mechanical analysis (DMA) equipment with a fixed tensile strain of 20% at different temperatures. Figure 1a shows the stress relaxation in the specimen at several different temperatures. The tensile stress in the stretched LCE reduced to 40% of the initial stress after 400 min at room temperature. While at high temperatures, the stress in a stretched LCE specimen could completely relax to zero after a while, similar to

DOI: 10.1021/acsami.7b09246
ACS Appl. Mater. Interfaces XXXX, XXX, XXX−XXX

the thermoplastic polymer. We further found that with the increase of temperature, the rate of stress relaxation increased dramatically. For instance, at 120 °C, it took 300 min for the specimen to relax to the stress-free state, whereas only 92 and 42 min were needed at 140 and 160 °C, respectively. The temperature-dependent stress relaxation in the LCE at high temperature is mainly originated from the bond exchanging reaction and the rearrangement of the polymer network. It is well-known that both associative and dissociative mechanisms may be involved in the exchangeable reaction of disulfide bonds.[34] On the basis of previous reports and our experimental results, we proposed that breakage of disulfide bonds could be continuously triggered by thermal energy under high temperature, which further generated free radicals and initiated an exchangeable reaction via an associative mechanism as shown in Figure 1c.[56] The time needed for the specimen to relax to the $1/e$ of the initially applied stress is commonly defined as the characteristic relaxation time τ. From the relationship between the characteristic time and temperature (inset of Figure 1a), we can conclude that the bond exchanging reaction in the disulfide LCE should slow down dramatically at 80 °C, which is about the upper limit of the working temperature of the LCE as a thermally actuated material. In another word, at 80 °C, the LCE with disulfide bonds behaves like a permanent cross-linked elastomer. In Figure 1a, it is also noted that at the beginning, the stress relaxation in the LCE was even faster at ambient temperature than that at 120 and 140 °C. We think that this phenomenon was mainly because of different stress relaxation mechanisms in the disulfide LCE at low and high temperature. At room temperature, the stress relaxation in the LCE was mainly because of the motion of polymer chains and the interactions between liquid crystal mesogens, whereas the dynamic bond exchanging reaction should be responsible for the stress relaxation in the LCE at high temperature. The time scale of the dynamic reaction of the disulfide bond at high temperature can be longer than the time scale of the motion of polymer chains at room temperature.

We also conducted stress relaxation tests of the LCE with a fixed tensile strain of 100% under UV illumination (Figure 1b). With such a large strain, the specimen was transparent and UV light could pass through it. During the test, the specimen (10 mm × 5 mm × 1 mm) was placed under the illumination of UV light with 365 nm wavelength. The power intensity of the UV light was 16.7 mW/cm^2. The stress in the stretched LCE with UV illumination gradually reduced to 25% of its initial stress, while the stress in the stretched LCE under laboratory fluorescent lighting in the lab could reach only 60% after 270 min. Such a difference confirmed that the exchange reaction of disulfide bonds in the LCE could also be activated by UV illumination at room temperature without requiring any catalysts or photoinitiators. This unique dynamic property of the LCE with disulfide bonds under UV illumination opens a new way for both spatial and temporal patterning of the director field of mesogens.

To study the influence of cross-linking density on the actuation behavior of the LCE, we synthesized three entries of the LCE film with different cross-linking densities as shown in Table 1. The cross-linking density of the LCE thin film could be easily controlled by adding a different amount of the cross-linking agent PETMP. We used simple extension tests to characterize mechanical properties of these LCE samples. The results are summarized in Figure S7 and Table 1. We calculated the tangential modulus of all the LCE samples when the engineering strain is 10%. The modulus decreased with the decrease of the cross-linking density. The rupturing strain increased from 350% for SS-LCE-1 with the highest cross-linking density to 1810% for SS-LCE-3 with the lowest cross-linking density.

Table 1. SS-LCE with Varied Cross-linking Density

sample	oligomer (mmol)	PETMP (mmol)	$E_{10\%}$ (MPa)	rupturing strain (%)
SS-LCE-1	3.6	1.8	0.12	350
SS-LCE-2	3.6	1.35	0.11	570
SS-LCE-3	3.6	0.9	0.05	1810

All the disulfide LCE pristine samples obtained from the hot compression appeared opaque and would transit to transparent without any observable deformation when heated to 80 °C, indicating that it was in the polydomain state. After being cooled to room temperature, the specimen recovered to the opaque state (Figure S8). Then, we prestretched all the disulfide LCE samples to 2 times their initial length and placed them under UV illumination for 1 h. After prestretch and UV illumination, the SS-LCE-1 sample with the highest cross-linking density showed a reversible contraction/expansion upon heating and cooling as shown in Figure 2a. The specimen was transparent at room temperature, indicating that the mesogenic molecules inside the LCE were well-aligned. Such a thermally induced reversible deformation clearly indicates that the LCE network was rearranged during the UV illumination process, which changed its permanent shape into the monodomain state.

A polarized optical microscope was used to confirm the alignment of liquid crystal mesogens. Because of the optical birefringence, the aligned LCE shows different brightness at varied angles with respect to the analyzer under the polarized optical microscope. In a polydomain LCE, the liquid crystal domains are randomly distributed. There is no brightness difference observed in the polydomain LCE at 45 and 90° with respect to the analyzer as shown in Figure S9. However, for a polydomain SS-LCE-1 upon mechanical stretching or the monodomain SS-LCE-1 specimen obtained after UV illumination, the maximum brightness can be observed at around 45° with respect to the analyzer, whereas the maximum darkness can be observed at 90°, which means that the LCE can be aligned by mechanical stretching and such an alignment can be fixed by UV illumination. When a monodomain LCE was heated up to 80 °C, we could not detect a brightness difference when we position the LCE sample at 45 and 90° with respect to the analyzer (Figure S9g,h). It indicates that the specimen transits from the monodomain to the isotropic state at high temperature.

After UV illumination, prestretched SS-LCE-2 and SS-LCE-3 could also stay in the stretched state without any externally applied stress. Both of them also contracted to their original length when heated to 80 °C. However, they could not expand after cooling down (Figures S10 and S11). It implies that the SS-LCE-2 and SS-LCE-3 specimens could not be fixed in the monodomain state under UV illumination and prestretched despite the same rearrangement of the polymer networks as that in SS-LCE-1. These results show that the cross-linking density has to be high enough to fix an LCE in the monodomain state. We propose the following reason for such an observation: after a disulfide LCE was stretched to the monodomain state under UV exposure, the bond exchanging

DOI: 10.1021/acsami.7b09246
ACS Appl. Mater. Interfaces XXXX, XXX, XXX−XXX

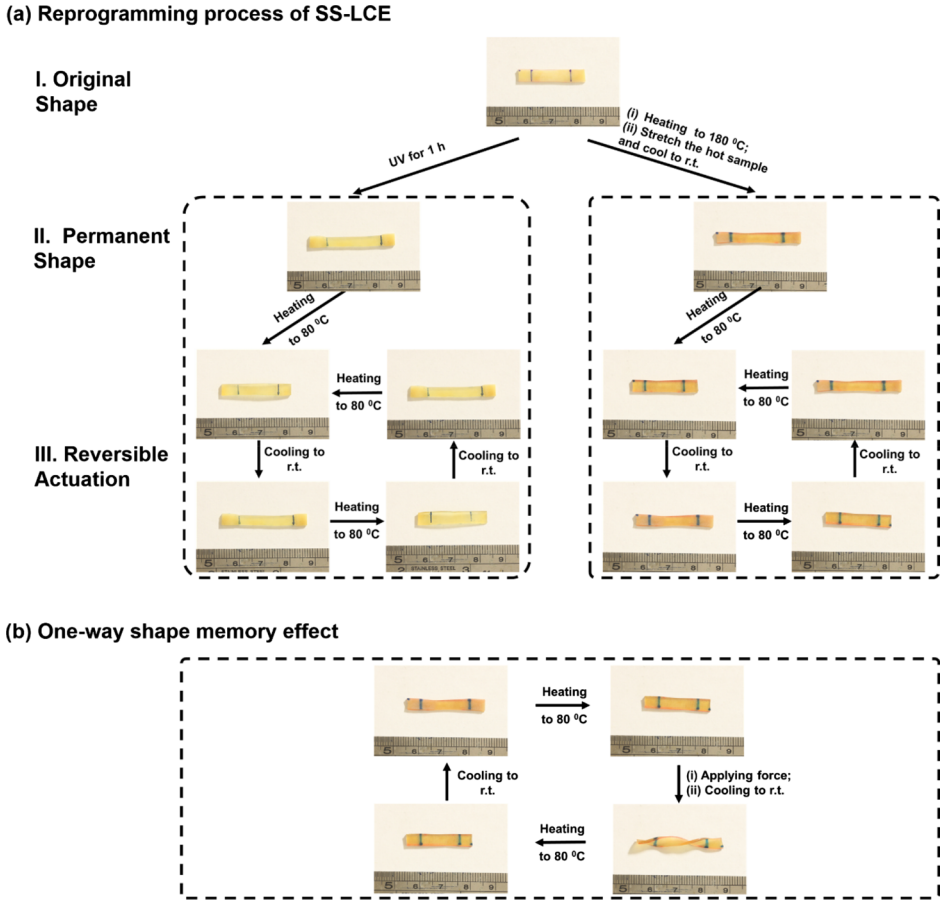

Figure 2. (a) Demonstration of the reprogrammable property of the SS-LCE-1 specimen either under UV irradiation or upon heating to 180 °C. The reshaped SS-LCE-1 specimen showed a reversible actuation behavior upon the heating/cooling process. (b) One-way shape memory effect of monodomain SS-LCE-1.

reaction happened, inducing the rearrangement of the polymer network and stress relaxation in the LCE. After the stress in a stretched LCE relaxed to zero, its elastic energy reached minimum. When heated above isotropic temperature, all three LCE samples contracted, and the elastic energy of the polymer network increased. When the samples were cooled down, the reduction of the elastic energy of the polymer network provided the driving force for the LCE going back to its initial monodomain state. When the cross-linking density was too low, the elastic energy reduction as the driving force was not large enough, and consequently, the polydomain LCE was formed at room temperature as shown in SS-LCE-2 and SS-LCE-3.

Besides UV reprogrammability, the LCE specimen could also rearrange its polymer network to the monodomain state under heating. In the experiment, the specimen was heated to 180 °C for 10 min and stretched to 2 times its initial length. The stretched specimen was then cooled down to room temperature. The thermally programmed specimen showed a similar actuating behavior as the UV programmed sample, as shown in Figure 2a. We further quantitatively studied the reversible actuating behavior of the LCE sample upon cyclic heating and cooling as shown in Figure S12. The actuating strain of UV and the thermally programmed monodomain LCE is around −25 and −20%, respectively. Both LCEs can maintain the reversible actuating behavior after tens of heating and cooling cycles (Figure S12). According to our knowledge, it is the first report of both UV and the thermally dual-reprogrammable LCE. The reprogrammable LCE specimen could also be locked into complex temporary shapes with a shape memory effect. As shown in Figure 2b, the same monodomain LCE specimen used in Figure 2a was heated above 80 °C. It contracted to the isotropic state. The specimen was then twisted to a helical shape by external torque and cooled down to room temperature. The interaction between mesogenic molecules locked the LCE in the twisted shape. The temporary twisted shape could be easily erased by additional heating and cooling cycles. The twisted sample would shorten and deform into a flat isotropic state. It then expanded and recovered to its permanent flat shape after cooling to room temperature.

Because of the exchanging reaction of disulfide bonds, the disulfide LCE can also be easily reprogrammed between the polydomain state and the monodomain state. In the experiment, we first stretched the as-prepared SS-LCE-1 sample under UV light for 1 h. The LCE sample can be fixed in the monodomain state and showed a reversible actuating behavior with an active strain around −20% upon heating and cooling (Figure S13a). We could easily change the monodomain LCE to the polydomain state by heating it up to 180 °C for 20 min and then cooling it down to room temperature. The free-standing polydomain LCE did not show any actuating behavior as demonstrated in Figure S13b. To obtain a free-standing monodomain LCE film again, we heated the polydomain LCE to 180 °C, stretched the hot sample, and cooled it down to room temperature. As expected, the LCE film showed a reversible actuating behavior as demonstrated in Figure S13c.

DOI: 10.1021/acsami.7b09246
ACS Appl. Mater. Interfaces XXXX, XXX, XXX−XXX

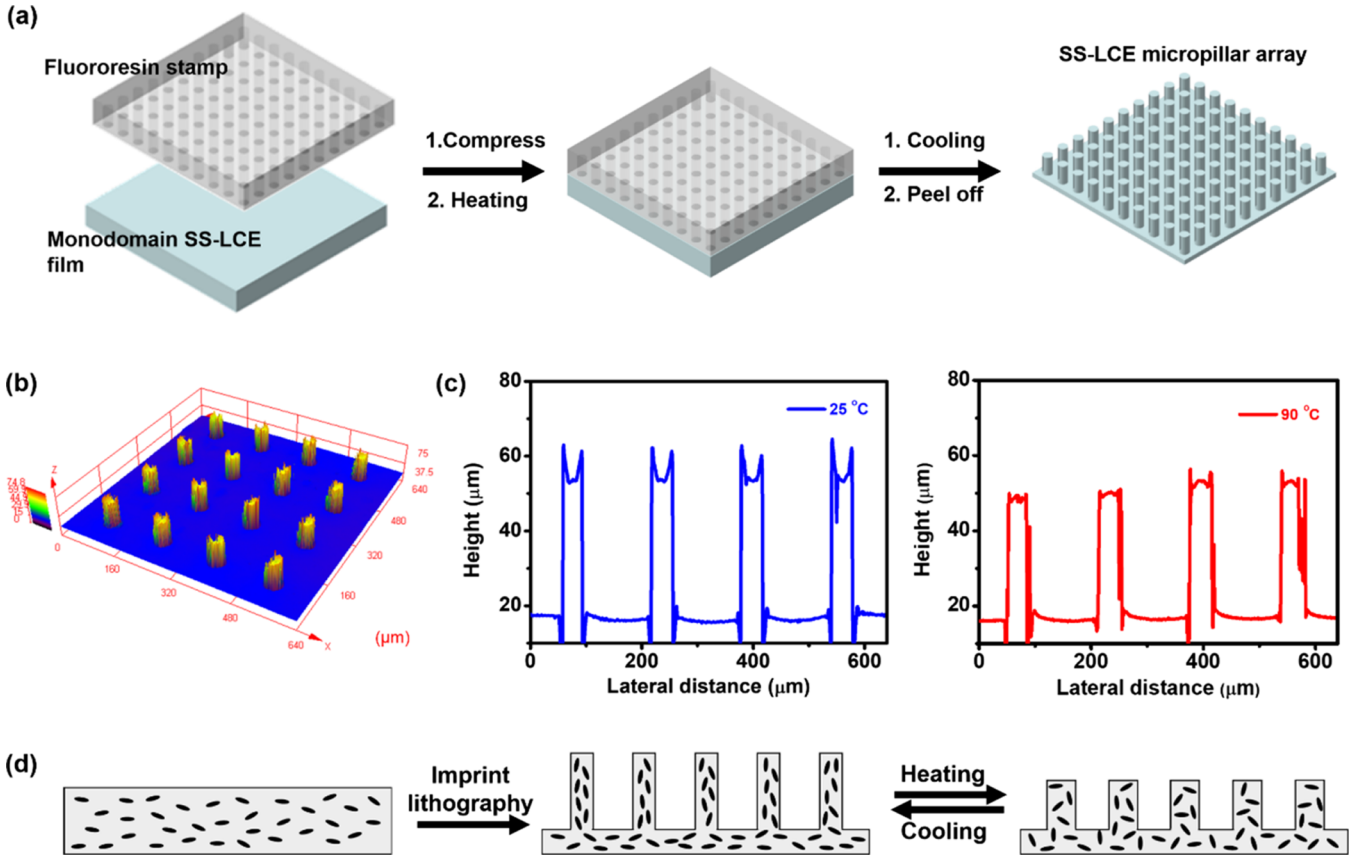

Figure 3. (a) Fabrication of the LCE micropillar array using imprint lithography. A monodomain LCE film was compressed with the fluororesin stamp mold and heated to 180 °C for 3 h. The LCE micropillar array was peeled off from the stamp mold after being cooled down; (b) confocal microscopy 3D image of the disulfide LCE micropillar array; (c) confocal microscopy profiles of the disulfide LCE micropillar pattern at 25 °C and upon being heated up to 90 °C; and (d) schematics of the evolution of mesogens in the LCE film during the imprinting process and with temperature variation.

All these experiments indicate that the disulfide LCE can be easily reprogrammed under UV light or upon heating.

Because of the reprogrammability of the LCE with the disulfide bond, we can fabricate an active micropillar array surface on an LCE film using fairly easy and robust imprint lithography, which can be hardly achieved using the LCE synthesized previously. The micropillar structure has recently attracted much attention because of its similarity to the functional biological systems such as gecko foot hairs[57−59] and lotus leaves[60−62] and so forth. Cui et al. used the magnetic field to align the liquid crystal mesogens and obtained a temperature-driven reversible gecko-like adhesive.[63] However, it is very challenging to scale-up magnetic-field assisted fabrication and make complex LCE microstructures. Herein, we used the reprogrammable SS-LCE-1 sample to fabricate active LCE micropillar arrays by imprint lithography. In the fabrication, the monodomain SS-LCE-1 film was compressed by a fluororesin stamp mold by clamps and heated at 180 °C for 3 h following the procedures reported previously (Figure 3a).[64−67] When the sample was cooled down, the LCE film was peeled off from the stamp mold and the film with the micropillar array replicating the fluororesin mold was obtained. Figure 3b shows the confocal microscopy image of the LCE micropillar array obtained from imprint lithography. It can be seen from Figure 3c that the micropillars have dimples on their top surfaces, which may be because of the flow behavior of the LCE during the hot embossing process.[68,69] In the as-prepared micropillar array, the pillars had an average height of 42.5 ± 0.6 μm and an average width of (38.4 ± 1.9) μm as shown in Figure 3c. When the LCE micropillar array was heated to 90 °C, the height of the pillars shortened to 35.0 ± 2.3 μm and the width expanded to 42.9 ± 1.5 μm, indicating that the liquid crystal mesogens were aligned along the longitudinal direction (Figure 3c). After being cooled down to room temperature, the pillars recovered to their initial size. Figure 3d sketches the evolution of mesogens in the LCE film during the imprinting process: an LCE film was initially in the monodomain state with uniformly oriented mesogens; when a stamp with arrays of cylindrical holes was pressed onto the LCE film at 180 °C, the LCE film behaved like a thermoplastic polymer and its surface was squeezed into the cylindrical holes; and because of the large shearing stress during the stamping, mesogens in the LCE entering into the stamp aligned along the longitudinal direction of the cylindrical holes and their orientation was fixed after being cooled down to room temperature and peeled off from the stamp. Consequently, the fabricated LCE micropillars could respond to temperature variation.

The exchangeable reaction of disulfide bonds also made the disulfide LCE self-healable. We cut an LCE to two pieces, put these two pieces in contact with each other, and heated them up to 180 °C for 3 h. The self-healed sample was then cooled down to room temperature. We stretched the self-healed specimen to 2 times its initial length and could not break it (Figure 4a). To study the self-healing efficiency of the disulfide

DOI: 10.1021/acsami.7b09246
ACS Appl. Mater. Interfaces XXXX, XXX, XXX−XXX

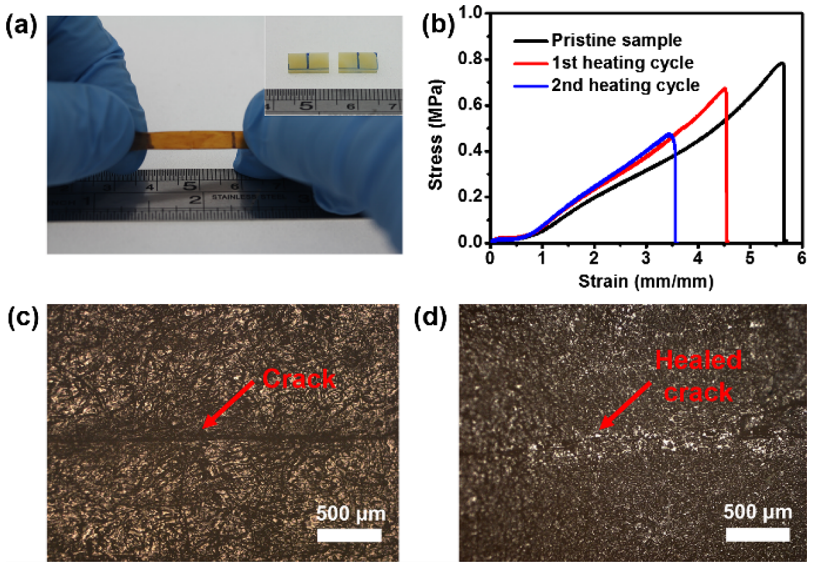

Figure 4. (a) Photograph of the stretched self-healed disulfide LCE. The self-healed specimen did not fail after stretching to 2 times its initial length. Inset: photograph of a broken SS-LCE-1 specimen. (b) stress−strain curves of the thermally healed disulfide LCE. The specimen was placed at 180 °C for 3 h for self-healing and microscopic images of the crack in LCE (c) before and (d) after heating at 180 °C for 3 h.

LCE sample, we conducted a simple extension test of the self-healed disulfide LCE specimen. Figure 4b shows the stress−strain curves of the specimen after cyclic breaking and healing under heating. The recovered rupturing strain was around 80% of the pristine sample for both the first and second cycle. The crack also disappeared after heating as observed by optical microscopy (Figure 4c,d). However, as shown in Figure S14, the self-healing efficiency was relatively low if the broken sample was placed under UV illumination. The rupturing strain of an initially broken sample after UV illumination for 3 h was only about 24% of the pristine sample. The irradiated sample also failed when stretched to 2 times its initial length, and the crack could not be completely healed under UV illumination (Figure S14). This is because in the experiment, we simply put two broken pieces of the LCE together without applying any additional force. At room temperature, the polymer chain mobility was low and the UV irradiation-induced disulfide exchange reaction could cause the healing of only the well-contacted area, whereas the area with a large separation between the two pieces could not be healed. Those unhealed areas were defects in the LCE, which could dramatically knock down its strength and rupturing strain.

The synthesized disulfide LCE also showed excellent durability because it could be reprogrammed without catalysts. For traditional vitrimer or vitrimer-like materials, a large amount of the catalyst is needed to promote the exchangeable reaction. However, no catalyst is needed in the disulfide metathesis reaction. As a result, the disulfide LCE could keep its reprogrammability even after being stored for 3 months. In the experiment, we stretched an SS-LCE-1 polydomain sample which has been stored for 3 months and placed it under UV irradiation for 1 h. The irradiated sample showed a reversible actuation behavior, exactly the same as the freshly prepared SS-LCE-1 samples (Figure S15).

CONCLUSION

In conclusion, we reported a newly developed, reprogrammable, reprocessible, and self-healable LCE with disulfide bonds. The disulfide bonds were exchangeable under either heating or UV illumination, which were utilized to align mesogenic molecules and change the permanent shape of an LCE. The aligned monodomain LCE could act as a soft actuating material with reversible contraction and expansion upon heating and cooling. The reprogrammable LCE could also be easily used for fabricating active structures with complex shapes such as arrays of micropillars. The disulfide LCE also showed good reprocessability, self-healing property, and excellent durability. Our study may not only develop a new reprogrammable, reprocessible, and self-healable LCE but also provide a deep understanding in designing the LCE as an actuating material.

Experimental Methods. Materials. (1,4-Bis-[4-(3-acryloyloxypropyloxy)benzoyloxy]-2-methylbenzene) (RM257) (Wilshire company, 95%), (2-hydroxyethoxy)-2-methylpropiophenone (HHMP, Sigma-Aldrich, 98%), EDDET (Sigma-Aldrich, 95%), PETMP (Sigma-Aldrich, 95%), dipropylamine (DPA, Sigma-Aldrich, 98%), 3% hydrogen peroxide solution (Sigma-Aldrich), sodium iodide (Sigma-Aldrich, 99%), and sodium thiosulfate pentahydrate (Fisher Scientific) were used as received without further purification.

Measurements. ^{1}H NMR was recorded on the 300 MHz 300 Bruker AVA instrument at room temperature with $CDCl_3$ as the solvent. Fourier-transformed infrared (FT-IR) spectra were measured on the Nicolet 6700 spectrometer (Thermo Scientific) with a liquid nitrogen-cooled MCT-A detector. TGA was carried out under the nitrogen flow at a heating rate of 10 °C/min on the Q600 SDT instrument (TA Instruments). DSC measurement was conducted on the Q100 DSC calorimeter (TA Instruments) in a nitrogen atmosphere. The sample was encapsulated in hermetically sealed aluminum pans. Hot compression was conducted on the Carver hot embossing system, with the operating temperature as 180° and the applied force as 1 ton. The mechanical property of the disulfide LCE films was measured using the Instron universal testing machine (5965 Dual Column Testing systems, Instron) with a 1000 N loading cell. The ends of the samples were glued onto acrylic plates which were clipped by the clamps of the Instron machine. The engineering strain rate was set at 0.5 min^{-1}. The

DOI: 10.1021/acsami.7b09246
ACS Appl. Mater. Interfaces XXXX, XXX, XXX−XXX

stress relaxation experiments under UV light were also measured on the Instron machine. The temperature-dependent stress relaxation experiments were measured by DMA using TA instrument DMA 2980. Images of crack healing were taken on the Axio microscope. The structure of the LCE micropillar array was acquired on the laser scanning confocal microscope (Olympus OLS4000).

Preparation of the Cross-linked SS-LCE Film. The SS-LCE was synthesized in the procedures shown in Scheme S1. First, RM257 (9.42 g, 16 mmol) and EDDET (3.64 g, 20 mmol) were dissolved in 50 mL acetone and then catalyst DPA (0.2 g, 2 mmol) was added into the solution. The mixture was stirred overnight and turned turbid. The upper solvent was poured and the lower viscous liquid was precipitated three times in methanol . After that, the precipitate was collected. The yield was 90%. The DP of the oligomer was calculated from the ^{1}H NMR spectrum. The signals around 8.15 ppm corresponded to the protons at the benzyl ring of RM257 and the integral was set as 4. The signals around 3.6 ppm which corresponded to the protons of the $-CH_2-$ near the oxygen atoms of EDDET were integrated as 9.69. The DP was calculated as $8/(9.69 - 8) = 4.7$. Then, the oligomer was dissolved in THF, and cross-linker PETMP (0.92 g, 1.8 mmol) was added into the solution. Then, oxidized reagent 3% hydrogen peroxide (10 mL) and catalyst NaI (0.02 g, 0.13 mmol) were added. The mixture was stirred for 24 h, and a yellow gel formed. The gel was cut into pieces and washed with 5% sodium thiosulfate solution. Gel pieces were then washed 3 times with water. The SS-LCE was obtained as white pieces after being dried at 85 °C in an oven overnight. Then, the particles of the SS-LCE were subjected to the Carver hot embossing system. The operating temperature was set as 180 °C, and the applied force was set as 1 ton. After 3 h, the film was cooled to room temperature by the water cooling system. Then, the LCE film with a smooth surface could be obtained. The cross-linking density was controlled by adding a different amount of cross-linking reagent PETMP.

Preparation of the Monodomain SS-LCE Film. The SS-LCE film obtained from the hot-compression process was in polydomain and appeared opaque. Both UV irradiation and heating could induce a rearrangement of the polymer network of the SS-LCE and align the film into the monodomain state. For the UV irradiation process, the film was stretched to 2 times its initial length and placed under 365 nm UV lamp for 1 h. The specimen recovered to 1.5 times the initial length after releasing the stretch. The specimen was heated and cooled cyclically to check the actuation behavior. For the heating process, the specimen was heated to 180 °C for 30 min and stretched. Then, the stretched specimen was cooled down to room temperature and heated to 80 °C to remove the plastic deformation during the cooling process. Then, the specimen was used for the actuation behavior test by cyclic heating and cooling.

Preparation of the Cross-linked LCE Film without Disulfide Bonds. The control sample of the cross-linked LCE film without disulfide bonds was prepared following procedures reported previously using two-step polymerization methods.[53,54] RM257 (10.9565 g, 18.6 mmol) was dissolved in toluene, and the mixture was heated at 85 °C to be homogeneous. Then, HHMP (0.0771 g, 0.3 mmol) was added into the solution and heated to be dissolved. After that, EDDET (2.736 g, 15 mmol) and PETMP (0.6996 g, 1.43 mmol) were added into the mixture dropwise. Then, the Michael addition reaction catalyst DPA (0.03779 g, 0.37 mmol) was added later. The mixture was degassed in vacuum to remove the bubbles inside and poured into a rectangular glass mold. The Michael addition reaction was taken under ambient temperature overnight. Then, after putting into the oven overnight to evaporate toluene, the film was placed under UV light (365 nm) for 15 min. The film was chopped into small pieces and used for hot compression.

■ ASSOCIATED CONTENT

Supporting Information

The Supporting Information is available free of charge on the ACS Publications website at DOI: 10.1021/acsami.7b09246.

Characterization results of the disulfide LCE using ^{1}H NMR, FT-IR, TGA, and DSC and tensile test and photographs of the actuation behavior of the disulfide LCE (PDF)

■ AUTHOR INFORMATION

Corresponding Author

*E-mail: shqcai@ucsd.edu.

ORCID

Zhijian Wang: 0000-0003-2929-8376

Notes

The authors declare no competing financial interest.

■ ACKNOWLEDGMENTS

S.C. acknowledges the support from National Science Foundation through grant no. CMMI-1554212 and ONR through grant no. N000141712062.

■ REFERENCES

(1) Thomsen, D. L.; Keller, P.; Naciri, J.; Pink, R.; Jeon, H.; Shenoy, D.; Ratna, B. R. Liquid Crystal Elastomers with Mechanical Properties of a Muscle. *Macromolecules* **2001**, *34*, 5868−5875.

(2) Camacho-Lopez, M.; Finkelmann, H.; Palffy-Muhoray, P.; Shelley, M. Fast Liquid-Crystal Elastomer Swims into the Dark. *Nat. Mater.* **2004**, *3*, 307−310.

(3) Woltman, S. J.; Jay, G. D.; Crawford, G. P. Liquid-Crystal Materials Find a New Order in Biomedical Applications. *Nat. Mater.* **2007**, *6*, 929−938.

(4) van Oosten, C. L.; Bastiaansen, C. W. M.; Broer, D. J. Printed Artificial Cilia from Liquid-Crystal Network Actuators Modularly Driven by Light. *Nat. Mater.* **2009**, *8*, 677−682.

(5) Gebhart, S. C.; Thompson, R. C.; Mahadevan-Jansen, A. Liquid-Crystal Tunable Filter Spectral Imaging for Brain Tumor Demarcation. *Appl. Opt.* **2007**, *46*, 1896−1910.

(6) Schuhladen, S.; Preller, F.; Rix, R.; Petsch, S.; Zentel, R.; Zappe, H. Iris-Like Tunable Aperture Employing Liquid-Crystal Elastomers. *Adv. Mater.* **2014**, *26*, 7247−7251.

(7) Wang, Z.; Fan, W.; He, Q.; Wang, Y.; Liang, X.; Cai, S. A Simple and Robust Way towards Reversible Mechanochromism: Using Liquid Crystal Elastomer as a Mask. *Extreme Mech. Lett.* **2017**, *11*, 42−48.

(8) Xing, H.; Li, J.; Shi, Y.; Guo, J.; Wei, J. Thermally Driven Photonic Actuator Based on Silica Opal Photonic Crystal with Liquid Crystal Elastomer. *ACS Appl. Mater. Interfaces* **2016**, *8*, 9440−9445.

(9) Castles, F.; Morris, S. M.; Hung, J. M. C.; Qasim, M. M.; Wright, A. D.; Nosheen, S.; Choi, S. S.; Outram, B. I.; Elston, S. J.; Burgess, C.; Hill, L.; Wilkinson, T. D.; Coles, H. J. Stretchable Liquid-Crystal Blue-Phase Gels. *Nat. Mater.* **2014**, *13*, 817−821.

(10) Tang, R.; Liu, Z.; Xu, D.; Liu, J.; Yu, L.; Yu, H. Optical Pendulum Generator Based on Photomechanical Liquid-Crystalline Actuators. *ACS Appl. Mater. Interfaces* **2015**, *7*, 8393−8397.

DOI: 10.1021/acsami.7b09246
ACS Appl. Mater. Interfaces XXXX, XXX, XXX−XXX

(11) Cheng, Z.; Wang, T.; Li, X.; Zhang, Y.; Yu, H. NIR–Vis–UV Light-Responsive Actuator Films of Polymer-Dispersed Liquid Crystal/Graphene Oxide Nanocomposites. *ACS Appl. Mater. Interfaces* **2015**, *7*, 27494–27501.
(12) Zhou, L.; Liu, Q.; Lv, X.; Gao, L.; Fang, S.; Yu, H. Photoinduced Triple Shape Memory Polyurethane Enabled by Doping with Azobenzene and GO. *J. Mater. Chem. C* **2016**, *4*, 9993–9997.
(13) Xie, P.; Zhang, R. Liquid Crystal Elastomers, Networks and Gels: Advanced Smart Materials. *J. Mater. Chem.* **2005**, *15*, 2529–2550.
(14) Yu, Y.; Ikeda, T. Soft Actuators Based on Liquid-Crystalline Elastomers. *Angew. Chem., Int. Ed.* **2006**, *45*, 5416–5418.
(15) Ikeda, T.; Mamiya, J.-i.; Yu, Y. Photomechanics of Liquid-Crystalline Elastomers and Other Polymers. *Angew. Chem., Int. Ed.* **2007**, *46*, 506–528.
(16) Ohm, C.; Brehmer, M.; Zentel, R. Liquid Crystalline Elastomers as Actuators and Sensors. *Adv. Mater.* **2010**, *22*, 3366–3387.
(17) Lv, J.-a.; Liu, Y.; Wei, J.; Chen, E.; Qin, L.; Yu, Y. Photocontrol of Fluid Slugs in Liquid Crystal Polymer Microactuators. *Nature* **2016**, *537*, 179–184.
(18) Liu, L.; Geng, B.; Sayed, S. M.; Lin, B.-P.; Keller, P.; Zhang, X.-Q.; Sun, Y.; Yang, H. Single-layer Dual-phase Nematic Elastomer Films with Bending, Accordion-Folding, Curling and Buckling Motions. *Chem. Commun.* **2017**, *53*, 1844–1847.
(19) Buguin, A.; Li, M.-H.; Silberzan, P.; Ladoux, B.; Keller, P. Micro-actuators: When Artificial Muscles Made of Nematic Liquid Crystal Elastomers Meet Soft Lithography. *J. Am. Chem. Soc.* **2006**, *128*, 1088–1089.
(20) Yang, H.; Buguin, A.; Taulemesse, J.-M.; Kaneko, K.; Méry, S.; Bergeret, A.; Keller, P. Micron-Sized Main-Chain Liquid Crystalline Elastomer Actuators with Ultralarge Amplitude Contractions. *J. Am. Chem. Soc.* **2009**, *131*, 15000–15004.
(21) Spillmann, C. M.; Naciri, J.; Ratna, B. R.; Selinger, R. L. B.; Selinger, J. V. Electrically Induced Twist in Smectic Liquid–Crystalline Elastomers. *J. Phys. Chem. B* **2016**, *120*, 6368–6372.
(22) Donnio, B.; Wermter, H.; Finkelmann, H. A Simple and Versatile Synthetic Route for the Preparation of Main-Chain, Liquid-Crystalline Elastomers. *Macromolecules* **2000**, *33*, 7724–7729.
(23) Wang, L.; Liu, W.; Guo, L.-X.; Lin, B.-P.; Zhang, X.-Q.; Sun, Y.; Yang, H. A Room-Temperature Two-Stage Thiol–Ene Photoaddition Approach towards Monodomain Liquid Crystalline Elastomers. *Polym. Chem.* **2017**, *8*, 1364–1370.
(24) Küpfer, J.; Finkelmann, H. Nematic Liquid Single Crystal Elastomers. *Makromol. Chem., Rapid Commun.* **1991**, *12*, 717–726.
(25) Ahir, S. V.; Tajbakhsh, A. R.; Terentjev, E. M. Self-Assembled Shape-Memory Fibers of Triblock Liquid-Crystal Polymers. *Adv. Funct. Mater.* **2006**, *16*, 556–560.
(26) Pei, Z.; Yang, Y.; Chen, Q.; Terentjev, E. M.; Wei, Y.; Ji, Y. Mouldable Liquid-Crystalline Elastomer Actuators with Exchangeable Covalent Bonds. *Nat. Mater.* **2014**, *13*, 36–41.
(27) Yang, Y.; Pei, Z.; Zhang, X.; Tao, L.; Wei, Y.; Ji, Y. Carbon Nanotube–Vitrimer Composite for Facile and Efficient Photo-Welding of Epoxy. *Chem. Sci.* **2014**, *5*, 3486–3492.
(28) Pei, Z.; Yang, Y.; Chen, Q.; Wei, Y.; Ji, Y. Regional Shape Control of Strategically Assembled Multishape Memory Vitrimers. *Adv. Mater.* **2016**, *28*, 156–160.
(29) Yang, Y.; Pei, Z.; Li, Z.; Wei, Y.; Ji, Y. Making and Remaking Dynamic 3D Structures by Shining Light on Flat Liquid Crystalline Vitrimer Films without a Mold. *J. Am. Chem. Soc.* **2016**, *138*, 2118–2121.
(30) Chen, Q.; Yu, X.; Pei, Z.; Yang, Y.; Wei, Y.; Ji, Y. Multi-Stimuli Responsive and Multi-Functional Oligoaniline-Modified Vitrimers. *Chem. Sci.* **2017**, *8*, 724–733.
(31) Montarnal, D.; Capelot, M.; Tournilhac, F.; Leibler, L. Silica-Like Malleable Materials from Permanent Organic Networks. *Science* **2011**, *334*, 965–968.
(32) Capelot, M.; Montarnal, D.; Tournilhac, F.; Leibler, L. Metal-Catalyzed Transesterification for Healing and Assembling of Thermosets. *J. Am. Chem. Soc.* **2012**, *134*, 7664–7667.
(33) Capelot, M.; Unterlass, M. M.; Tournilhac, F.; Leibler, L. Catalytic Control of the Vitrimer Glass Transition. *ACS Macro Lett.* **2012**, *1*, 789–792.
(34) Denissen, W.; Winne, J. M.; Du Prez, F. E. Vitrimers: Permanent Organic Networks with Glass-like Fluidity. *Chem. Sci.* **2016**, *7*, 30–38.
(35) Ware, T. H.; McConney, M. E.; Wie, J. J.; Tondiglia, V. P.; White, T. J. Voxelated Liquid Crystal Elastomers. *Science* **2015**, *347*, 982–984.
(36) Ying, H.; Zhang, Y.; Cheng, J. Dynamic Urea Bond for the Design of Reversible and Self-Healing Polymers. *Nat. Commun.* **2014**, *5*, 3218.
(37) Zheng, N.; Fang, Z.; Zou, W.; Zhao, Q.; Xie, T. Thermoset Shape-Memory Polyurethane with Intrinsic Plasticity Enabled by Transcarbamoylation. *Angew. Chem., Int. Ed.* **2016**, *55*, 11421–11425.
(38) Taynton, P.; Yu, K.; Shoemaker, R. K.; Jin, Y.; Qi, H. J.; Zhang, W. Heat- or Water-Driven Malleability in a Highly Recyclable Covalent Network Polymer. *Adv. Mater.* **2014**, *26*, 3938–3942.
(39) Taynton, P.; Ni, H.; Zhu, C.; Yu, K.; Loob, S.; Jin, Y.; Qi, H. J.; Zhang, W. Repairable Woven Carbon Fiber Composites with Full Recyclability Enabled by Malleable Polyimine Networks. *Adv. Mater.* **2016**, *28*, 2904–2909.
(40) Lei, Z. Q.; Xiang, H. P.; Yuan, Y. J.; Rong, M. Z.; Zhang, M. Q. Room-Temperature Self-Healable and Remoldable Cross-Linked Polymer Based on the Dynamic Exchange of Disulfide Bonds. *Chem. Mater.* **2014**, *26*, 2038–2046.
(41) Li, L.; Feng, W.; Welle, A.; Levkin, P. A. UV-Induced Disulfide Formation and Reduction for Dynamic Photopatterning. *Angew. Chem.* **2016**, *128*, 13969–13973.
(42) Fairbanks, B. D.; Singh, S. P.; Bowman, C. N.; Anseth, K. S. Photodegradable, Photoadaptable Hydrogels via Radical-Mediated Disulfide Fragmentation Reaction. *Macromolecules* **2011**, *44*, 2444–2450.
(43) Canadell, J.; Goossens, H.; Klumperman, B. Self-Healing Materials Based on Disulfide Links. *Macromolecules* **2011**, *44*, 2536–2541.
(44) Pepels, M.; Filot, I.; Klumperman, B.; Goossens, H. Self-Healing Systems Based on Disulfide–Thiol Exchange Reactions. *Polym. Chem.* **2013**, *4*, 4955–4965.
(45) Lu, Y.-X.; Guan, Z. Olefin Metathesis for Effective Polymer Healing via Dynamic Exchange of Strong Carbon–Carbon Double Bonds. *J. Am. Chem. Soc.* **2012**, *134*, 14226–14231.
(46) Lu, Y.-X.; Tournilhac, F.; Leibler, L.; Guan, Z. Making Insoluble Polymer Networks Malleable via Olefin Metathesis. *J. Am. Chem. Soc.* **2012**, *134*, 8424–8427.
(47) Cromwell, O. R.; Chung, J.; Guan, Z. Malleable and Self-Healing Covalent Polymer Networks through Tunable Dynamic Boronic Ester Bonds. *J. Am. Chem. Soc.* **2015**, *137*, 6492–6495.
(48) Scott, T. F.; Schneider, A. D.; Cook, W. D.; Bowman, C. N. Photoinduced Plasticity in Cross-Linked Polymers. *Science* **2005**, *308*, 1615–1617.
(49) Kloxin, C. J.; Scott, T. F.; Park, H. Y.; Bowman, C. N. Mechanophotopatterning on a Photoresponsive Elastomer. *Adv. Mater.* **2011**, *23*, 1977–1981.
(50) Michal, B. T.; Jaye, C. A.; Spencer, E. J.; Rowan, S. J. Inherently Photohealable and Thermal Shape-Memory Polydisulfide Networks. *ACS Macro Lett.* **2013**, *2*, 694–699.
(51) Otsuka, H.; Nagano, S.; Kobashi, Y.; Maeda, T.; Takahara, A. A Dynamic Covalent Polymer Driven by Disulfide Metathesis under Photoirradiation. *Chem. Commun.* **2010**, *46*, 1150–1152.
(52) Han, G.; Nie, J.; Zhang, H. Facile Preparation of Recyclable Photodeformable Azobenzene Polymer Fibers with Chemically Crosslinked Network. *Polym. Chem.* **2016**, *7*, 5088–5092.
(53) Yakacki, C. M.; Saed, M.; Nair, D. P.; Gong, T.; Reed, S. M.; Bowman, C. N. Tailorable and Programmable Liquid-Crystalline Elastomers Using a Two-Stage Thiol–Acrylate Reaction. *RSC Adv.* **2015**, *5*, 18997–19001.

DOI: 10.1021/acsami.7b09246
ACS Appl. Mater. Interfaces XXXX, XXX, XXX–XXX

(54) Ahn, C.; Liang, X.; Cai, S. Inhomogeneous Stretch Induced Patterning of Molecular Orientation in Liquid Crystal Elastomers. *Extreme Mech. Lett.* **2015**, *5*, 30−36.
(55) Saed, M. O.; Torbati, A. H.; Starr, C. A.; Visvanathan, R.; Clark, N. A.; Yakacki, C. M. Thiol-Acrylate Main-Chain Liquid-Crystalline Elastomers with Tunable Thermomechanical Properties and Actuation Strain. *J. Polym. Sci., Part B: Polym. Phys.* **2017**, *55*, 157−168.
(56) Tobolsky, A. V.; MacKnight, W. J.; Takahashi, M. Relaxation of Disulfide and Tetrasulfide Polymers. *J. Phys. Chem.* **1964**, *68*, 787−790.
(57) King, D. R.; Bartlett, M. D.; Gilman, C. A.; Irschick, D. J.; Crosby, A. J. Creating Gecko-Like Adhesives for "Real World" Surfaces. *Adv. Mater.* **2014**, *26*, 4345−4351.
(58) Wang, Y.; Tian, H.; Shao, J.; Sameoto, D.; Li, X.; Wang, L.; Hu, H.; Ding, Y.; Lu, B. Switchable Dry Adhesion with Step-Like Micropillars and Controllable Interfacial Contact. *ACS Appl. Mater. Interfaces* **2016**, *8*, 10029−10037.
(59) Hu, H.; Tian, H.; Shao, J.; Li, X.; Wang, Y.; Wang, Y.; Tian, Y.; Lu, B. Discretely Supported Dry Adhesive Film Inspired by Biological Bending Behavior for Enhanced Performance on a Rough Surface. *ACS Appl. Mater. Interfaces* **2017**, *9*, 7752−7760.
(60) Chandra, D.; Yang, S. Stability of High-Aspect-Ratio Micropillar Arrays against Adhesive and Capillary Forces. *Acc. Chem. Res.* **2010**, *43*, 1080−1091.
(61) Li, X.; Tian, H.; Shao, J.; Ding, Y.; Liu, H. Electrically Modulated Microtransfer Molding for Fabrication of Micropillar Arrays with Spatially Varying Heights. *Langmuir* **2013**, *29*, 1351−1355.
(62) Chen, C.-M.; Yang, S. Directed Water Shedding on High-Aspect-Ratio Shape Memory Polymer Micropillar Arrays. *Adv. Mater.* **2014**, *26*, 1283−1288.
(63) Cui, J.; Drotlef, D.-M.; Larraza, I.; Fernández-Blázquez, J. P.; Boesel, L. F.; Ohm, C.; Mezger, M.; Zentel, R.; del Campo, A. Bioinspired Actuated Adhesive Patterns of Liquid Crystalline Elastomers. *Adv. Mater.* **2012**, *24*, 4601−4604.
(64) Shao, J.; Ding, Y.; Tang, Y.; Liu, H.; Lu, B.; Cui, D. A Novel Overlay Process for Imprint Lithography Using Load Release and Alignment Error Pre-Compensation Method. *Microelectron. Eng.* **2008**, *85*, 168−174.
(65) Shao, J.; Liu, H.; Ding, Y.; Wang, L.; Lu, B. Alignment Measurement Method for Imprint Lithography Using Moiré Fringe Pattern. *Opt. Eng.* **2008**, *47*, 113604.
(66) Shao, J. Y.; Ding, Y. C.; Liu, H. Z.; Wang, L.; Yin, L.; Shi, Y. S.; Jiang, W. T. Strategy for a Loading Force Induced Overlay Position Shift in Step Imprint Lithography. *Proc. Inst. Mech. Eng., Part B* **2009**, *223*, 9−17.
(67) Wang, C.; Shao, J.; Tian, H.; Li, X.; Ding, Y.; Li, B. Q. Step-Controllable Electric-Field-Assisted Nanoimprint Lithography for Uneven Large-Area Substrates. *ACS Nano* **2016**, *10*, 4354−4363.
(68) Heyderman, L. J.; Schift, H.; David, C.; Gobrecht, J.; Schweizer, T. Flow Behaviour of Thin Polymer Films Used for Hot Embossing Lithography. *Microelectron. Eng.* **2000**, *54*, 229−245.
(69) Scheer, H.-C.; Schulz, H. A Contribution to the Flow Behaviour of Thin Polymer Films during Hot Embossing Lithography. *Microelectron. Eng.* **2001**, *56*, 311−332.

DOI: 10.1021/acsami.7b09246
ACS Appl. Mater. Interfaces XXXX, XXX, XXX−XXX